[Prion 3:2, 99-109; April/May/June 2009]; ©2009 Landes Bioscience

Research Paper

Comparative prion disease gene expression profiling using the prion disease mimetic, cuprizone

Laura R. Moody,[1,2] Allen J. Herbst,[2,3] Han Sang Yoo,[4] Joshua P. Vanderloo[2] and Judd M. Aiken[1-3,*]

[1]Program in Cellular and Molecular Biology; and [2]Comparative Biosciences; School of Veterinary Medicine; University of Wisconsin; Madison, WI USA; [3]Centre for Prions and Protein Folding Diseases; University of Alberta; Edmonton, AB CA; [4]College of Veterinary Medicine; KRF Zoonotic Disease Priority Research Institute and BK21 for Veterinary Science; Seoul National University; Seoul, Korea

Abbreviations: RML, rocky mountain lab; TSE, transmissible spongiform encephalopathy; i.p., intraperitoneal; DPI, days post-inoculation; RMA, robust multi-array average; qPCR, quantitative PCR; Gfap, glial fibrillary acidic protein; Tbp, TATA box binding protein; GO, gene ontology

Key words: RML infection, cuprizone, microarray, gene expression, comparative profiling

Identification of genes expressed in response to prion infection may elucidate biomarkers for disease, identify factors involved in agent replication, mechanisms of neuropathology and therapeutic targets. Although several groups have sought to identify gene expression changes specific to prion disease, expression profiles rife with cell population changes have consistently been identified. Cuprizone, a neurotoxicant, qualitatively mimics the cell population changes observed in prion disease, resulting in both spongiform change and astrocytosis. The use of cuprizone-treated animals as an experimental control during comparative expression profiling allows for the identification of transcripts whose expression increases during prion disease and remains unchanged during cuprizone-triggered neuropathology. In this study, expression profiles from the brains of mice preclinically and clinically infected with Rocky Mountain Laboratory (RML) mouse-adapted scrapie agent and age-matched controls were profiled using Affymetrix gene arrays. In total, 164 genes were differentially regulated during prion infection. Eighty-three of these transcripts have been previously undescribed as differentially regulated during prion disease. A 0.4% cuprizone diet was utilized as a control for comparative expression profiling. Cuprizone treatment induced spongiosis and astrocyte proliferation as indicated by glial fibrillary acidic protein (*Gfap*) transcriptional activation and immunohistochemistry. Gene expression profiles from brain tissue obtained from cuprizone-treated mice identified 307 differentially regulated transcript changes. After comparative analysis, 17 transcripts unaffected by cuprizone treatment but increasing in expression from preclinical to clinical prion infection were identified. Here we describe the novel use of the prion disease mimetic, cuprizone, to control for cell population changes in the brain during prion infection.

*Correspondence to: Judd Aiken; Centre for Prions and Protein Folding Diseases; University of Alberta; Edmonton, AB T6G 2M8 CA; Tel.: +780.248.1722; Fax: +780.492.9352; Email: jmaiken@ualberta.ca

Submitted: 03/20/09; Accepted: 05/19/09

Previously published online as a *Prion* E-publication:
http://www.landesbioscience.com/journals/prion/article/9059

Introduction

Transmissible spongiform encephalopathies (TSEs) or prion diseases are infectious, neurodegenerative conditions that are inevitably fatal. Human TSEs include Creutzfeldt-Jakob disease, Gerstmann-Sträussler-Scheinker syndrome, fatal familial insomnia and kuru. Animal TSEs include scrapie in sheep, bovine spongiform encephalopathy ("mad cow disease") in cattle, chronic wasting disease in cervids, and transmissible mink encephalopathy. Common pathological features shared by TSEs include spongiform vacuolation, gliosis and neuronal loss.[1] These characteristic changes may also be accompanied by the accumulation of amyloid plaques in the neuropil of infected brains.

Several groups have identified individual genes that are highly expressed during prion disease, typically using subtractive hybridization of cDNA libraries or microarray analysis. RNA expression profiles have been developed for many different TSE strains at different stages during infection.[2-17] Many of these RNA expression profiles were generated from whole brain homogenates from clinically affected animals. Early in the disease process, low-grade microglia and astrocytes are activated. As a result, these cells proliferate, progressively amplifying during infection,[18,19] changing the cell population of the brain. This neuroinflammation is a generalized reaction that occurs in many brain diseases including Alzheimer disease,[20] Parkinson disease[21] and multiple sclerosis,[22] among others. Not surprisingly, most of the RNAs differentially regulated during TSE infection are related to activated astrocytes and microglia. RNA changes resulting from inflammation mask transcript changes associated with prion disease-specific neuropathology. Greenwood et al. (2005) addressed this problem by developing RNA expression profiles from neuronal cell lines that are persistently infected with TSE agent,[23] identifying a

number of neuronal transcripts associated with prion disease (clusterin—associated with the clearing of cellular debris and apoptosis; metallothionein 1—inhibits oxidative damage and apoptosis) and several transcripts not previously identified in other studies. The ability to focus on neuronal changes in a brain infection would be an important progression of this line of research.

We hypothesized that gene profiling of animals treated with the prion disease mimetic, cuprizone, would allow us to identify transcripts associated with cell population changes, providing greater focus to those transcripts related to prion pathogenesis. Cuprizone (bis-cyclohexanone-oxaldihydraxone) is a copper chelator which, when fed to mice, produces demyelination in the central nervous system.[24] Demyelination occurs soon after cuprizone dosing, exclusively affecting oligodendrocytes.[25] Pattison and Jebbett observed that mice, fed a diet supplemented with 0.4% cuprizone, developed histopathological lesions in the brain very similar to those induced by murine TSE agent.[26] Both cuprizone treatment and TSEs exhibit extracellular vacuolation, astrocytosis and astrocyte hypertrophy in the white matter of the cerebellum, midbrain and cerebellar peduncles. Additionally, cuprizone treatment, like prion disease, induces microglial activation and recruitment[27] without loss of the blood-brain barrier.[28] As cuprizone treatment causes neuroinflammation similar to prion disease, it provides a useful model system for identifying transcripts associated with broad neuroinflammation in the absence of the prion-specific PrP^{TSE}. Here we report the use of cuprizone as a control for transcriptional events associated with neuroinflammation, facilitating the identification of several novel transcripts upregulated during a prion infection.

Results

Identification of previously undescribed transcripts differentially regulated during prion disease. Microarray analysis was performed to detect differences in gene expression in the mouse brain at three time points during prion infection. C57BL/6 mice were intraperitoneally infected with RML-infected mouse brain homogenate and sacrificed at 108 dpi, 158 dpi and at the presentation of clinical disease (198 dpi), with age-matched, mock-inoculated controls at each time point. At 108 and 158 dpi, no clinical symptoms were present, however, protease-resistant PrP was detected at both 158 and 198 dpi (Fig. 2I, L and O).

RNA samples were obtained from brain samples at all three time points and differentially regulated genes were identified using microarray analysis. The RMA method was used to background correct, normalize and summarize gene expression probe set data (representing individual genes) to identify differentially-expressed genes at each time point during prion disease. Differentially regulated genes were filtered on expression (10.0–99.0th expression percentile) to control for extreme or minimal signal intensity. Following statistical analysis (described in Materials and Methods), 164 genes were identified as being differentially regulated during prion disease. Many of these changes have been identified previously[2-17] and include several transcripts known to be associated with proliferating astrocytes and microglia, such as cystatin F (leukocystatin), lymphocyte antigen 86, cathepsin S, CD53 antigen, CD68 antigen and glial fibrillary acidic protein. Supplemental Table 2 includes all 164 differentially regulated transcripts identified during our prion time course analysis. Our analysis, however, detected 83 transcripts that have not previously been identified as differentially expressed during prion disease, likely due to our lowering of the threshold of detection from the usual ≥2-fold to ≥1.5-fold. It should be noted that all transcripts identified as differentially expressed were deemed statistically significant changes. These transcripts were analyzed using the Gene Ontology (GO) classification system. The majority of transcripts identified have not yet been classified, however, 27 were found to be categorized in a variety of biological processes (Table 1). Genes related to the immune response and response to stimulus GO-terms were strongly represented, including genes encoding for guanylate binding proteins (*Gbp3*, *Gbp6*) and interferon-induced proteins (*Ifi35*, *Ifitm1*, *Rsad2*). Genes involved in protein modification and intracellular cellular signaling were also upregulated. Several genes downregulated during prion disease belong to the ubiquitin cycle and cellular developmental processes.

Neuroinflammatory changes induced by prion disease and cuprizone treatment. Oral dosing of mice with the copper chelator cuprizone was used to generate chronic astrocytosis similar to that seen during prion disease. To define the impact of cuprizone treatment, we initiated a time course study of the prion disease mimetic, cuprizone. Cuprizone-treated mice were age-matched to the mice used for our prion studies, then orally dosed for 3, 4, 6, 7, 8 or 10 weeks with 0.4% cuprizone, with untreated age-matched mice used as controls. To determine the most appropriate cuprizone treatment (i.e., treatment time that mimics prion pathology most closely), quantitative PCR (qPCR) was used to measure astrocyte-specific glial fibrillary acidic protein (*Gfap*) expression levels during prion time courses and cuprizone treatment (Fig. 1). As expected during prion disease, *Gfap* expression increased over the course of infection. With cuprizone treatment, *Gfap* expression peaked after seven weeks of treatment and reached a plateau after eight weeks. During clinical disease prion infection (198 dpi), *Gfap* abundance was approximately 12-fold above the *Gfap* levels measured in uninfected animals and 5-times higher than the *Gfap* measured in the cuprizone-treated animals (Fig. 1). At 158 dpi, *Gfap* levels were comparable to those observed in the 8 and 10 week cuprizone treated brains suggesting an equivalent amount of astrocytosis. The eight week cuprizone treatment was selected for gene expression analysis.

Spongiform vacuolation and astrocytosis were compared in the cuprizone-treated and prion-infected brains. Following H&E staining of brain slices from cuprizone-treated mice, vacuoles were observed in the white matter and granular layer of the cerebellum as well as in the pons and frontal cortex (Fig. 2A and D). During prion disease, vacuoles were first observed in the cerebellum and midbrain at 158 dpi with spongiosis becoming more prevalent in the cerebellum, midbrain and frontal cortex at clinical disease (Fig. 2J and M). Robust astrocytosis was observed, immunohistochemically, using an antibody for the detection of astrocyte-specific GFAP, in the frontal cortex, thalamus, corpus callosum and interposed nucleus (Fig. 2E) in cuprizone-treated

Table 1 **Previously unidentified, differentially regulated gene expression changes in RML-infected brain tissue**

Probe set ID	Gene symbol	Gene title	108 dpi	158 dpi	198 dpi
Immune Response					
1431591_s_at	Isg15	ISG15 ubiquitin-like modifier	1.2	2.3	2.1
1418392_a_at	Gbp3	guanylate binding protein 3	1.2	1.8	1.7
1426397_at	Tgfbr2	transforming growth factor, beta receptor II	1.1	1.2	1.7
1424617_at	Ifi35	interferon-induced protein 35	1.1	1.6	1.6
1451318_a_at	Lyn	Yamaguchi sarcoma viral (v-yes-1) oncogene homolog	1.4	1.4	1.6
1425156_at	Gbp6	guanylate binding protein 6	1.1	1.7	1.5
1418641_at	Lcp2	lymphocyte cytosolic protein 2	1.0	1.6	1.4
Intracellular Signaling Cascade					
1460287_at	Timp2	tissue inhibitor of metalloproteinase 2	1.3	1.6	2.6
1460188_at	Ptpn6	protein tyrosine phosphatase, non-receptor type 6	1.6	1.9	2.4
1455132_at	A430107D22Rik	RIKEN cDNA A430107D22 gene	1.5	1.5	1.4
1452398_at	Plce1	phospholipase C, epsilon 1	1.1	1.3	1.6
1438936_s_at	Ang	angiogenin, ribonuclease, RNase A family, 5	1.0	1.4	1.9
1428479_at	Nfatc1	nuclear factor of activated T-cells, cytoplasmic, calcineurin-dependent 1	1.6	1.3	1.4
1416675_s_at	Plcd1	phospholipase C, delta 1	1.6	1.2	1.2
Protein Modification Process					
1418191_at	Usp18	ubiquitin specific peptidase 18	1.5	3.6	3.9
1451584_at	Havcr2	hepatitis A virus cellular receptor 2	1.3	1.8	2.1
1416340_a_at	Man2b1	mannosidase 2, alpha B1	1.5	1.4	1.7
1449342_at	Ptplb	protein tyrosine phosphatase-like (proline instead of catalytic arginine), member b	-1.1	1.4	1.5
1433768_at	Palld	palladin, cytoskeletal associated protein	1.3	1.1	1.5
Response to Stimulus					
1423547_at	Lyz2	lysozyme 2	1.8	3.4	5.5
1421009_at	Rsad2	radical S-adenosyl methionine domain containing 2	1.3	2.1	2.2
1424254_at	Ifitm1	interferon induced transmembrane protein 1	-1.1	1.7	1.1
Ubiquitin Cycle					
1433664_at	Ube2q2	ubiquitin-conjugating enzyme E2Q (putative) 2	-1.3	-1.3	-1.5
1419562_at	Birc6	baculoviral IAP repeat-containing 6	-1.8	-1.2	-1.3
Cellular Developmental Process					
1437947_x_at	Vdac1	voltage-dependent anion channel 1	-1.2	-1.7	-1.3
1453134_at	Pik3ca	phosphatidylinositol 3-kinase, catalytic, alpha polypeptide	-1.7	-1.4	-1.3
1449044_at	Eef1e1	eukaryotic translation elongation factor 1 epsilon 1	-1.7	1.0	-1.1
Other					
1448891_at	Fcrls	Fc receptor-like S, scavenger receptor	2.2	2.0	2.8
1421457_a_at	Samsn1	SAM domain, SH3 domain and nuclear localization signals, 1	1.3	1.9	2.3
1451655_at	Slfn8	schlafen 8	1.1	1.8	2.3
1418825_at	Irgm	immunity-related GTPase family, M	1.2	2.0	2.3
1420591_at	Gpr84	G protein-coupled receptor 84	1.4	1.7	2.2
1424754_at	Ms4a7	membrane-spanning 4-domains, subfamily A, member 7	-1.0	1.3	2.1
1443698_at	Xaf1	XIAP associated factor 1	1.1	1.8	2.1
1436346_at	Cd109	CD109 antigen	1.1	-1.1	2.1
1449227_at	Ch25h	cholesterol 25-hydroxylase	1.1	1.6	2.0
1451564_at	Parp14	poly (ADP-ribose) polymerase family, member 14	1.4	1.9	2.0
1421408_at	Igsf6	immunoglobulin superfamily, member 6	1.2	1.3	2.0
1454757_s_at	D12Ertd647e	DNA segment, Chr 12, ERATO Doi 647, expressed	1.2	1.7	1.9
1451537_at	Chi3l1	chitinase 3-like 1	1.1	1.7	1.8
1419879_s_at	Trim25	tripartite motif-containing 25	1.2	1.3	1.8

Table 1 **Previously unidentified, differentially regulated gene expression changes in RML-infected brain tissue (continued)**

1456133_x_at	Itgb5	integrin beta 5	1.5	1.3	1.8
1421374_a_at	Fxyd1	FXYD domain-containing ion transport regulator 1	-1.6	1.4	1.8
1448561_at	Ncf2	neutrophil cytosolic factor 2	1.4	1.6	1.8
1451132_at	Pbxip1	pre-B-cell leukemia transcription factor interacting protein 1	1.3	1.3	1.8
1426454_at	Arhgdib	Rho, GDP dissociation inhibitor (GDI) beta	1.1	1.7	1.7
1449591_at	Casp4	caspase 4, apoptosis-related cysteine peptidase	1.0	1.5	1.7
1434945_at	Lpcat2	lysophosphatidylcholine acyltransferase 2	1.2	1.3	1.7
1450234_at	Ms4a6c	membrane-spanning 4-domains, subfamily A, member 6C	1.3	1.7	1.7
1460351_at	S100a11	S100 calcium binding protein A11 (calgizzarin)	-1.6	1.4	1.7
1422571_at	Thbs2	thrombospondin 2	1.2	1.3	1.6
1429525_s_at	Myo1f	myosin IF	1.2	1.5	1.6
1418099_at	Tnfrsf1b	tumor necrosis factor receptor superfamily, member 1b	1.2	1.4	1.6
1458019_at		Mus musculus Transcribed locus	1.0	1.4	1.6
1424829_at	A830007P12Rik	RIKEN cDNA A830007P12 gene	1.3	1.2	1.5
1454748_at	Naprt1	nicotinate phosphoribosyltransferase domain containing 1	1.6	1.3	1.5
1451139_at	Slc39a4	solute carrier family 39 (zinc transporter), member 4	1.3	1.1	1.5
1437886_at	Klhl6	kelch-like 6 (Drosophila)	1.2	1.3	1.5
1420624_a_at	Vamp8	vesicle-associated membrane protein 8	-1.5	1.2	1.3
1421221_at	Bco2	beta-carotene oxygenase 2	1.3	1.5	1.3
1449960_at	Nptx2	neuronal pentraxin 2	-1.2	1.5	1.3
1418451_at	Gng2	guanine nucleotide binding protein (G protein), gamma 2	-1.5	1.1	1.2
1424058_at	Prrc1	proline-rich coiled-coil 1	1.5	1.1	1.2
1427903_at	Phpt1	phosphohistidine phosphatase 1	-1.7	1.1	1.1
1419812_s_at	Ccdc56	coiled-coil domain containing 56	-1.6	1.1	1.0
1426187_a_at	Hax1	HCLS1 associated X-1	-1.6	1.1	1.0
1417653_at	Pvalb	parvalbumin	-2.6	1.0	1.0
1435522_a_at	2310016E02Rik	RIKEN cDNA 2310016E02 gene	-2.0	1.1	1.0
1428464_at	Ndufa3	NADH dehydrogenase (ubiquinone) 1 alpha subcomplex, 3	-2.1	1.1	1.0
1416979_at	Pomp	proteasome maturation protein	-1.6	1.1	1.0
1424122_s_at	Commd1	COMM domain containing 1	-1.7	1.2	-1.0
1416277_a_at	Rplp1	ribosomal protein, large, P1	-1.6	1.1	-1.0
1450818_a_at	Ndufa7	NADH dehydrogenase (ubiquinone) 1 alpha subcomplex, 7 (B14.5a)	-1.5	1.1	-1.0
1452790_x_at	Ndufa3	NADH dehydrogenase (ubiquinone) 1 alpha subcomplex, 3	-2.0	1.0	-1.0
1427102_at	Slfn4	schlafen 4	1.1	1.8	-1.0
1434391_at	Hnrnpu	Heterogeneous nuclear ribonucleoprotein U	-1.7	1.1	-1.0
1418083_at	0610009B22Rik	RIKEN cDNA 0610009B22 gene	-1.5	-1.0	-1.1
1442887_at	AI853363	expressed sequence AI853363	-1.7	-1.0	-1.2
1422884_at	Snrpd3	small nuclear ribonucleoprotein D3	-1.7	1.5	-1.4
1428570_at	Ccnc	cyclin C	-1.5	-1.4	-1.4
1450770_at	3632451O06Rik	RIKEN cDNA 3632451O06 gene	-1.3	-1.4	-1.5
1417121_at	Gabra6	gamma-aminobutyric acid (GABA-A) receptor, subunit alpha 6	-1.1	-1.3	-1.6
1433452_at	B630019K06Rik	RIKEN cDNA B630019K06 gene	-1.1	-1.5	-1.6

Transcripts were subjected to the Gene Ontology classification system for discovery of biological processes affected by prion disease. Fold change vs. control at three time points are shown here.

animals. In prion-infected animals, basal astrocyte levels were observed at 108 dpi, with astrocyte levels rising throughout the brain at 158 and 198 dpi (Fig. 2H, K and N), consistent with the expression of *Gfap* observed by qPCR.

PrP^{TSE} was not observed in the brains of either mock-infected or cuprizone-treated mice when assayed for immunohistochemically (Fig. 2C and F). Although PrP^{TSE} was not observed in brain samples from infected animals at 108 dpi, punctate staining was

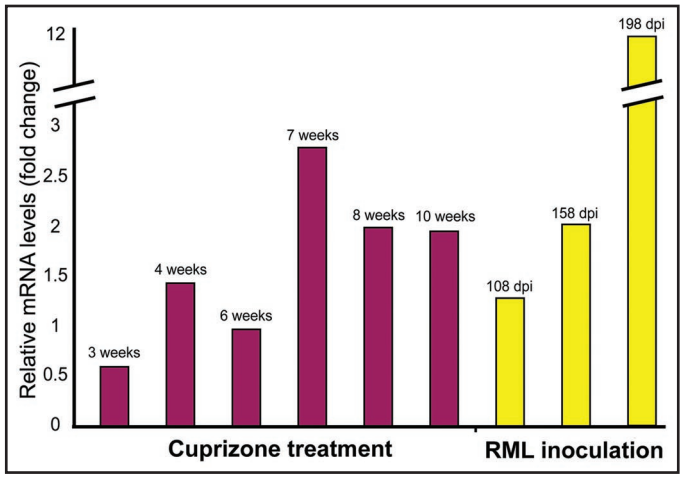

Figure 1. Expression of *Gfap* during cuprizone treatment and prion disease. Relative *Gfap* mRNA levels from 3, 4, 6, 7, 8 and 10 weeks of cuprizone treatment and 108, 158 and 198 dpi RML infection were generated by the Pfaffl method after qPCR, as indicated by fold change versus age-matched controls. After 8 and 10 weeks of cuprizone intoxication, *Gfap* levels most closely resemble those observed at 158 dpi of prion disease. *Tbp* was used as an endogenous control for normalization.

observed, at 158 dpi, in the pons and medulla and, at clinical stage, in the pons, medulla, midbrain, thalamus and frontal cortex (Fig. 2I, L and O).

Cuprizone treatment induces differential gene expression. Microarray analysis identified 319 genes differentially expressed in mouse brain after eight weeks of cuprizone treatment. Of these, 307 transcripts were grouped according to their functional annotations (Fig. 3). The majority of upregulated transcripts were associated with two biological processes; (1) immune system (including inflammatory response) and (2) metabolic processes. Immune system genes that were upregulated include chemokine (C-C motif) ligands, Fc receptors, and components of the complement system. Metabolic process genes included proteolytic cathepsins (C, D, H, L, S and Z), and lysosymes 1 and 2. Other upregulated genes were related to the regulation of apoptosis, cell communication, cellular adhesion and localization. Of the genes downregulated during cuprizone treatment, several genes play a role in axon ensheathement (proteolipid protein (myelin)1 and claudin 11), likely due to the demyelinating effects of cuprizone.

In a simple comparison of the gene expression profiles of mice infected with prion disease and those treated with cuprizone, 54% (88 of 164) of the transcripts differentially expressed during prion disease were also differentially expressed following cuprizone treatment. These transcripts include 28 genes associated with the immune system, eight genes involved with cell death, and five genes associated in lipid metabolism. It is clear that similar molecular mechanisms exist during prion disease and cuprizone treatment, presumably due to the activation of astrocytes and microglia in both, as well as the death of specific cell types (e.g., neurons during prion disease, oligodendrocytes during cuprizone treatment), which lead to spongiform vacuoles upon histological examination. Conversely, 231 of the genes upregulated by cuprizone treatment were not induced by prion disease, suggesting that stress response pathways activated during cuprizone treatment may be compromised during prion infection.

Comparative analysis of prion-infected gene expression profiles and gene expression profiles associated with cuprizone treatment. To identify transcripts related to prion disease and unchanged during cuprizone-induced neuroinflammation, probe sets from the prion disease time course experiment were re-analyzed (see Materials and Methods). One cluster emerged containing transcripts that increased in expression over the time course of prion disease (Fig. 4A). The transcripts in this cluster were statistically assessed, producing 333 transcripts which were increasing in expression over the course of prion disease. In parallel, probe sets from the cuprizone data set were also filtered on expression and a transcript with no expression change between control and cuprizone treatment was identified (TATA box binding protein—*Tbp*). Transcripts with 100–85% similarity were recognized, using the Euclidean similarity metric (Fig. 4B), producing 22,729 transcripts that were unchanged during cuprizone treatment. Analysis of both the cluster containing transcripts increasing in expression over the course of prion disease and the unchanging cuprizone data set identified 17 transcripts that were present in both data sets. These represent transcripts upregulated during prion disease but remained unchanging following cuprizone treatment (Fig. 4C). In total, 14 of the 17 transcripts were annotated. Two of the genes upregulated during prion disease are involved in the neuropeptide signaling, triggered by a peptide neurotransmitter binding to a cell surface receptor. These transcripts and their $\log_2$ transformed expression ratios are shown in Figure 5. Full gene names and fold change versus control values are available in Supplemental Table 3.

Validation of microarray data. To independently validate the gene expression data generated by our microarray experiments, qPCR was used to measures the expression of three genes identified as upregulated: radical S-adenosyl methionine domain containing 2 (*Rsad2*) which was previously unreported as upregulated during prion disease, as well as apolipoprotein D (*ApoD*) and suppressor of cytokine signaling 3 (*Socs3*) which were upregulated in prion disease and not during cuprizone treatment. Both *ApoD*[8,11,13,16] and *Socs3*,[14] have been previously described in prion disease gene array studies, and *ApoD* has been a useful gene for validation via qPCR.[11] QPCR analyses used the same total RNA samples as used for initial microarray studies. For all genes examined, expression levels found by microarray analysis were confirmed, although, in general, we observed higher relative fold-change levels with qPCR than microarray analysis. This has been described as a common phenomenon, though trends remain consistent across assays.[33] The general expression pattern of each transcript was confirmed, validating the expression results we obtained from microarray analysis (Fig. 6).

Discussion

We identified novel transcripts differentially regulated during prion disease, transcripts differentially regulated after eight weeks of treatment with 0.4% cuprizone as well as transcripts

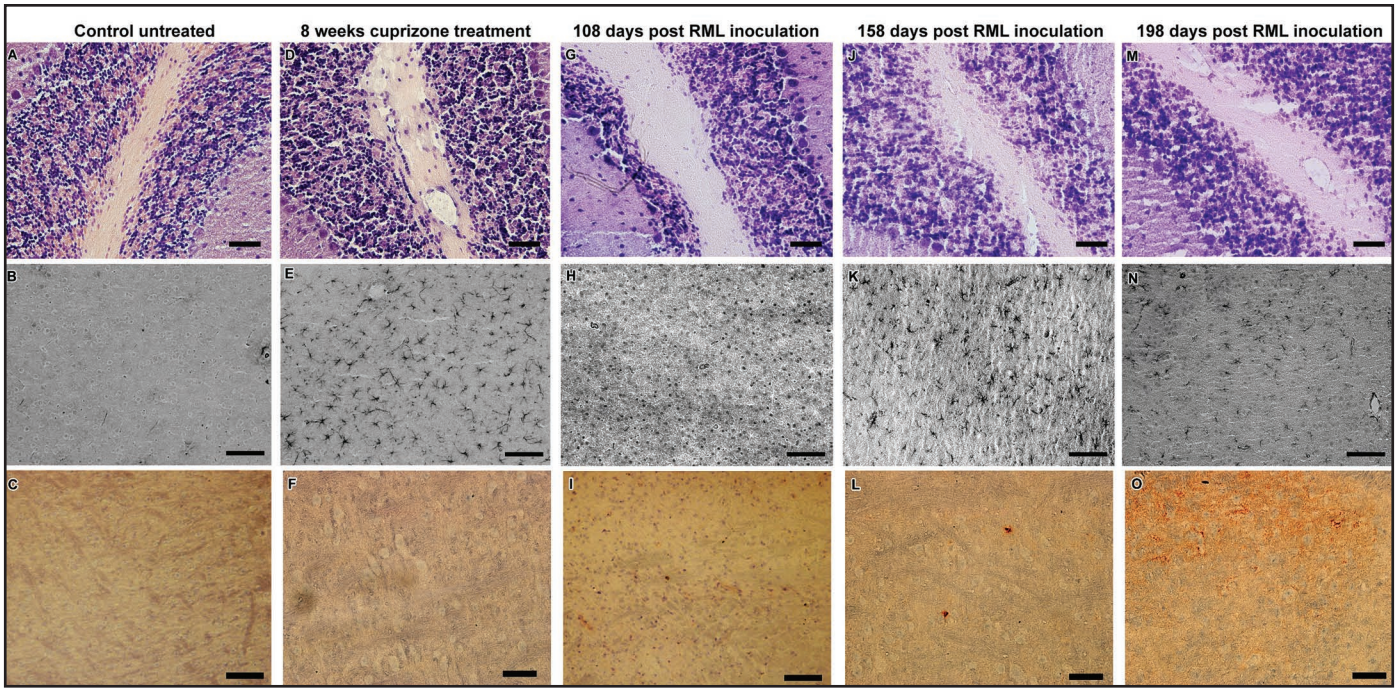

Figure 2. Spongiosis and astrocytosis in mice treated with cuprizone, infected with RML or controls. (A, D, G, J and M) Hematoxylin and eosin staining shows spongiosis in the white matter of the cerebellum after eight weeks of cuprizone treatment and after 158 and 198 days of RML infection. (B, E, H, K and N) Anti-GFAP immunohistochemistry shows star-shaped astrocytosis in the frontal cortex after cuprizone treatment and after 158 and 198 days of RML infection. (C, F, I, L and O) PrP^{TSE} staining in the medulla. Red, positive staining can be seen at 158 and 198 dpi and is not observed after cuprizone treatment. Scale bars: (A, D, G, J, M, F, L and O) = 50 μm; (B, E, H, K, N, C and I) = 100 μm.

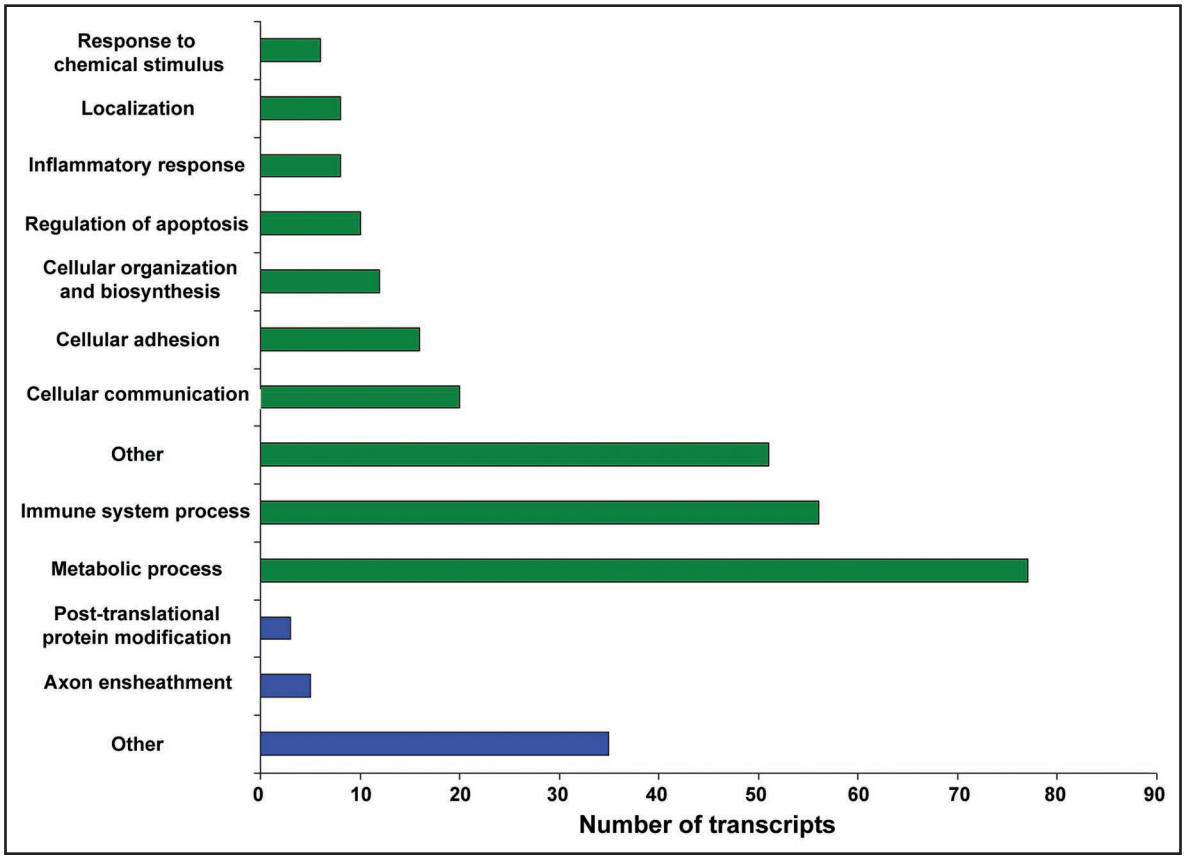

Figure 3. For figure legend, see page 105.

Figure 3. Functional analysis of transcripts differentially regulated in the brains of mice treated with cuprizone. The DAVID annotational database was utilized to determine which gene ontology biological processes were affected by cuprizone treatment ($p \leq 0.05$). Upregulated transcripts are in green; downregulated transcripts are in blue.

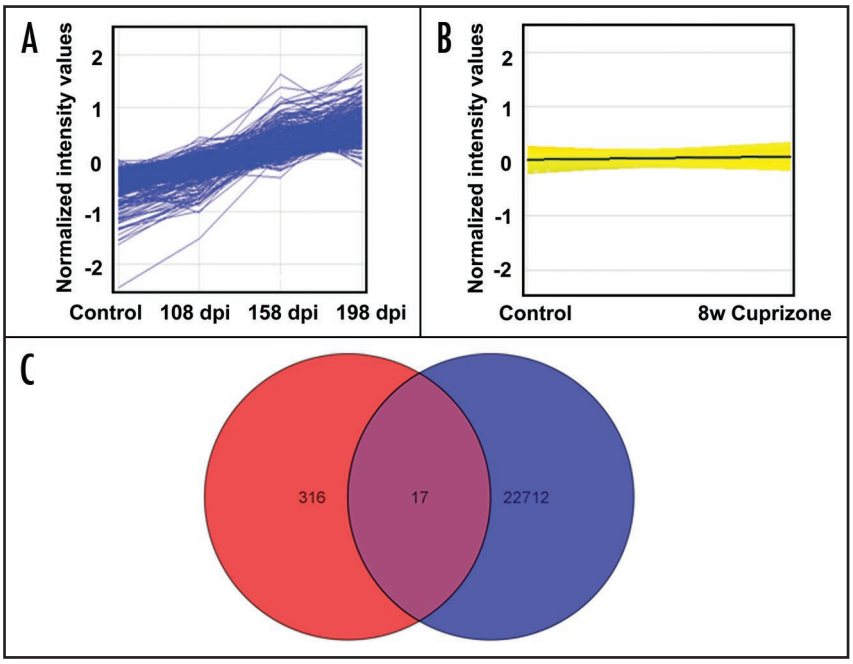

Figure 4. Comparative analysis between transcripts increasing in expression during prion disease and unchanging during cuprizone treatment. (A) After SOM clustering analysis, one cluster emerged containing transcripts that increased in expression over the time course of prion infection (shown here, 333 total transcripts). (B) The cuprizone data set was mined for one transcript whose expression was unchanged as compared to control (*Tbp*). Using the Euclidean similarity metric, transcripts with 100–85% similar expression patterns to *Tbp* were identified (22,729 total transcripts). (C) Venn diagram illustrating the comparative gene expression analysis of both data sets described above. In total, 17 probe sets belonged to both data sets and represent transcripts whose expression increased during prion disease but did not change with cuprizone treatment. This overlap signifies transcripts whose expression is related to prion disease and not associated to the changing cell population that occurs during neuroinflammation.

upregulated during mouse-adapted prion disease that were unchanged during cuprizone-induced neuroinflammation.

Several studies have been undertaken to identify gene expression changes associated with prion disease.[2-17] We identified many prion disease-induced transcripts that had been reported previously including *Gfap,* several cathepsins, components of the complement system, many Fc receptors, *Cst7*, *Serpina3n*, *Lgals3*, *CD84*, *CD68* and *CD52*. Another 83 previously unidentified differentially regulated genes were identified during preclinical and clinical RML prion infection. This increase in the number of gene expression changes is likely due to the use of the Affymetrix Mouse Genome 430 2.0 Array, a more comprehensive mouse genome expression microarray than previously used and the inclusion of transcripts with a differential expression of ≥1.5 fold. Many of the transcripts that had been newly described as downregulated in response to prion infection (Table 1) were not present in our differentially regulated cuprizone dataset. The comparative analysis of the transcripts increasing in expression over the course of prion disease and unchanging with cuprizone treatment removed all of the downregulated transcripts from the analysis. Future investigation is necessary to determine if these gene changes are unique to prion disease and what their downregulation means for understanding prion pathology.

The upregulation of several transcripts related to the immune response GO-term suggests the response of immune cells in the brain to prion infection. At 158 dpi, many immune response related transcripts are upregulated ≥1.5-fold. When C57Bl/6 mice are inoculated i.p. with the RML prion agent, T-cells do not infiltrate the brain until the breakdown of the blood-brain barrier, 185 dpi[34] and prion disease does not illicit an antibody-based immune response.[35] Therefore, the upregulated transcripts related to the immune response GO-term are not expected to be associated with activated T-cells. It is likely that these transcripts are expressed by astrocytes and microglia, which are proliferating during preclinical infection. The expression of two of these genes, *lsg15* and *Lyn*, is upregulated during astrocytosis in other systems; *Isg15* is expressed by astrocytes following viral infection[36] and *Lyn* is reported to be expressed by microglia after stimulation with beta-amyloid.[37]

We report the first gene expression analysis of brain tissue from mice treated with 0.4% cuprizone treatment. The use of 0.2% cuprizone as a demyelinating agent has been described previously and gene expression studies have been undertaken, but the neuropathological similarities to prion disease have only been described when the intake of cuprizone is ≥0.4%.[26] The gene expression profile in response to cuprizone treatment described here is distinct and more robust than previous studies.[38-41] Fifty-six transcripts reported as upregulated during cuprizone treatment are related to the immune response GO-term, many of which are also upregulated during prion disease, including *Clec7a*, *Ccl3*, *Ccl6*, *Gp49a*, parts of the classical complement system, several murine MHC components, and activated microglial markers like *CD68* and *Ly86*. In addition, many transcripts involved in the regulation of apoptosis were also upregulated during cuprizone treatment, likely due to the demyelination process that selectively targets oligodendrocytes. More than seventy transcripts upregulated during cuprizone treatment were annotated as involved in metabolic processes, including several cathepsins, *Hexa*, *Hexb* and lysozymes. The upregulation of these transcripts is likely due to the breaking down of both cuprizone and the cellular remnants of oligodendrocytes undergoing apoptosis.

The use of cuprizone as a control for comparative gene expression analysis is a novel technique facilitating the identification of

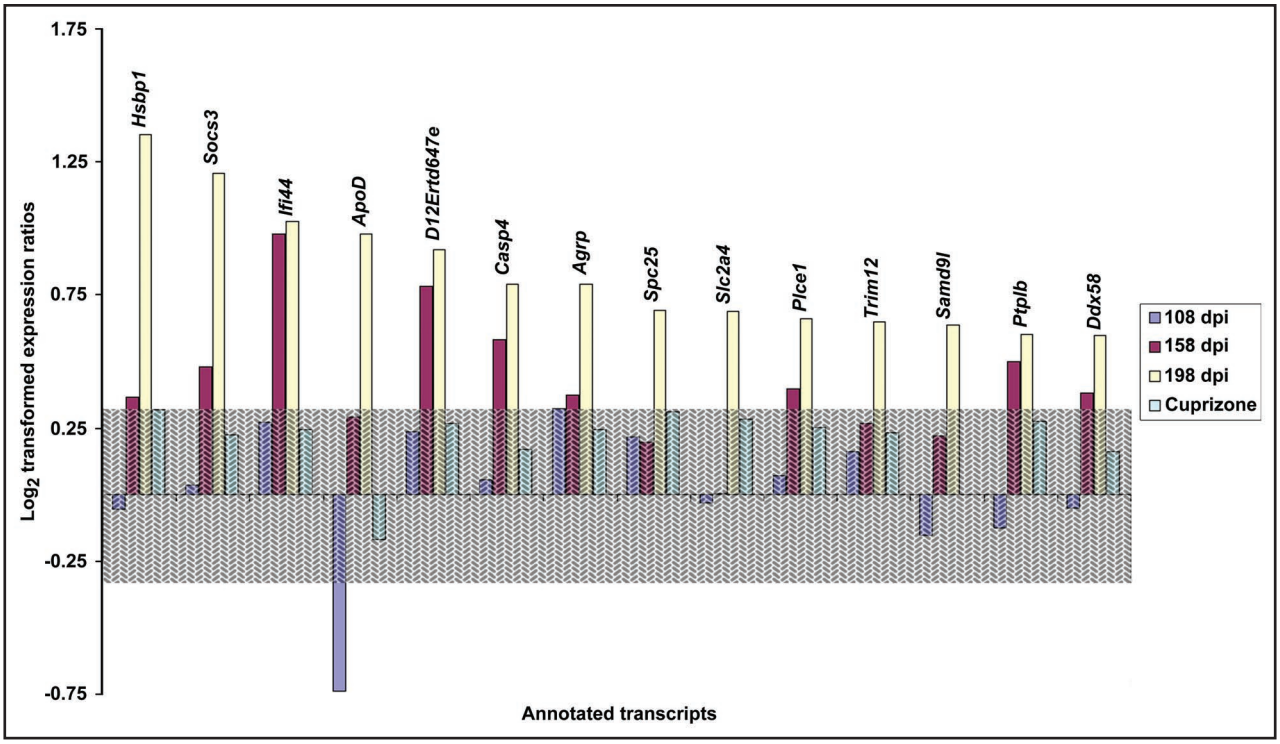

Figure 5. Annotated transcripts upregulated during prion disease and unrelated to cuprizone-induced neuroinflammation. Of the seventeen transcripts that increased in expression over the course of prion disease and remained unchanged during cuprizone treatment, fourteen were found to be annotated. The $\log_2$ transformed expression ratios versus control are shown here for ease in visualization, allowing gene expression to be centered on zero. The shaded region represents non-significant, unchanging transcript levels. Unchanging was classified as 10.0–0.31 $\log_2$ transformed expression ratio versus control.

prion disease-specific transcript changes that are not related to the robust neuroinflammation observed during prion disease. By identifying transcripts whose expression increases during prion disease but remain unchanged with cuprizone treatment, transcript changes related to the changing cell population in the brain during neuroinflammation (i.e., proliferation of astrocytes and microglia) could be removed. In previous gene expression studies, known markers for astrocytes and microglia were among the most upregulated transcripts identified. While these changes are important for understanding the state of the brain during prion disease, they may mask important gene expression changes related to prion pathogenesis. Similarities are clearly present between prion disease and its mimetic, cuprizone, making it a useful control for comparative gene expression analysis. In total, 14 annotated transcripts were identified as increasing in expression during prion disease and not related to the neuroinflammatory profile associated with cuprizone treatment. To note, nine of these transcripts (*Hsbp1, Socs3, Ifi44, D12Ertd647e, Casp4, Agrp, Plce1, Ptpbl, Ddx58)* were upregulated preclinically and may provide insights into the progressive impairment of the CNS during prion infection.

We identified signaling pathways that may be important to prion pathogenesis. Transcripts upregulated during prion disease but not during cuprizone treatment fell into two signaling pathways. The products of *Plce1* and *Agrp* are both involved in the neuropeptide signaling pathway. PLCE1 hydrolyses various polyphosphoinositides that activate the MAP kinase pathway, stimulating cell growth and differentiation.[42] PLCE1 may be involved in stimulating the proliferation of glial cells in the brain during prion infection. AGRP is a neuropeptide secreted by the hypothalamus that controls body weight.[43,44] AGRP also plays a role in adipocytokine signaling, another signaling pathway found to be represented in our data by AGRP, SLC2A4 and SOCS3. Adipocytes, or fat cells, secrete numerous cytokines that are important for metabolic homeostasis and play a role in inflammation.[45] *Slc2a4* (also known as *Glut4*) codes for a glucose transporter found in muscle and adipose tissue whose transporter action is dependent upon insulin.[46] In adipocytes, SOCS3 works to suppress the expression of cytokines by inhibiting the JAK/STAT pathway in a negative feedback loop.[47] SOCS3, however, plays a role in numerous signaling cascades and its expression may not be related to adipocytokine signaling alone. The role of these pathways in prion infection as well as confirmation with protein data is currently being explored.

In summary, eighty-three previously undescribed, annotated transcripts have been identified that are differentially regulated in the mouse brain during RML prion disease. We have also reported 307 annotated transcripts that are differentially regulated in the brain after eight weeks of 0.4% cuprizone treatment. We have described a comparative analysis technique that has allowed us to identify transcripts that were upregulated over the course of prion disease but remained unchanged during cuprizone treatment. With this novel analysis tool, we identified 14 annotated transcripts that change in expression during prion disease and

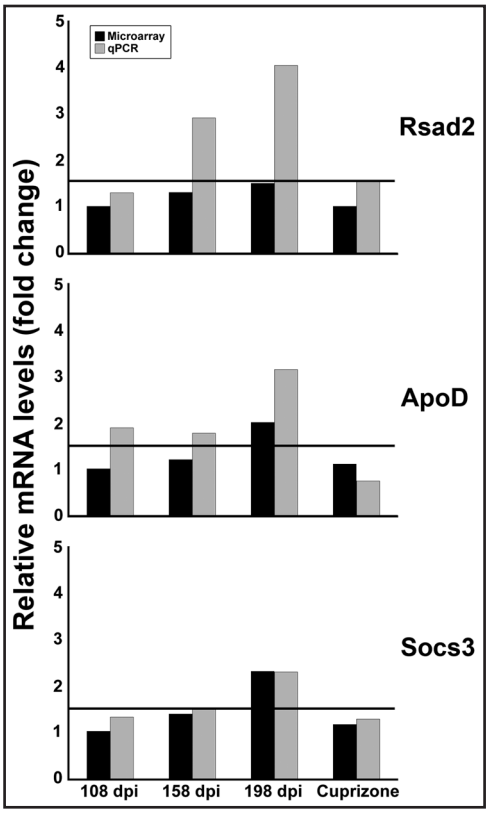

Figure 6. Validation of selected microarray results by qPCR. The expression of *Rsad2, ApoD* and *Socs3* was analyzed from RML-infected brain homogenate obtained at two preclinical time points (108 and 158 dpi) and at clinical disease (198 dpi) as well as after eight weeks of cuprizone treatment. Pooled RNA samples from eight infected/treated and eight controls were studied at each time point. The chart above shows relative mRNA levels, as indicated by fold change versus age-matched controls, generated by the Pfaffl method after qPCR, with a threshold line at 1.5-fold. *Tbp* was used as an endogenous control for normalization. Samples used for qPCR were from the same samples used for microarray analysis. Microarray data was taken from Table 1 and Supplemental Table 2.

do not appear to be related to the cell population changes occurring during disease. These transcripts may provide stepping stones for further investigation as to their roles in neurodegeneration and dysfunction during prion disease.

Materials and Methods

Animals and treatments. C57Bl/6 mice were intraperitoneally (i.p.) inoculated with 50 ul of a 10% brain homogenate (in PBS) prepared from a mouse clinically infected with the RML strain of TSE agent. Control mice were mock-inoculated with a 10% brain homogenate prepared from uninfected C57Bl/6 mice. Mice were sacrificed at two preclinical time points (108 and 158 days post-inoculation [dpi]) and at the appearance of clinical symptoms (198 dpi). For the cuprizone control, C57Bl/6 mice were fed chow supplemented with 0.4% cuprizone for 3, 4, 6, 7, 8 or 10 weeks, a dose at which no mortality was observed. These mice were age-matched to the mice used in our prion experiments in such a way that at the termination of each cuprizone treatment, the animals age would coincide with the onset of clinical disease in the prion infected mice. Control mice were fed a normal diet. Upon sacrifice, all brains were removed and bi-sected sagittally. One half was used for RNA isolation and gene expression analysis while the other half was embedded in Optimal Cutting Temperature medium (Tissue Tek O.C.T. Compound, Sakura Finetek, Torrance, CA), frozen in liquid nitrogen and stored at -80°C until sagittal sectioning.

RNA purification and array hybridization. Total RNA was purified from brain tissue (eight mice per treatment) using the Qiagen RNeasy Mini Kit protocol (Qiagen, Valencia, CA). cDNA was synthesized using the ImProm-II Reverse Transcription kit (Promega, Madison, WI) and an anchored T7-oligo(dT) V primer. Second strand synthesis was performed using DNA polymerase I (Invitrogen, Carlsbad, CA). Biotinylated cRNA was produced by in vitro transcription, incorporating biotin 14-CTP (Invitrogen, Carlsbad, CA) and biotin 16-UTP (Roche Applied Science, Indianapolis, IN) following manufacturer's instructions (Ambion, Austin, TX). Samples were hybridized onto Mouse Genome 430 2.0 Array (Affymetrix, Santa Clara, CA) at 45°C for 16 hours with a constant rotation at 60 rpm. The arrays were washed and stained using an Affymetrix fluidics station and scanned on an Affymetrix scanner. Each treatment array was performed in triplicate.

Data analysis. Raw microarray data was uploaded into the GeneSpring GX 9.0 Analysis Platform (Agilent, Santa Clara, CA). Microarray data was normalized and background corrected using Robust Multi-Array Average (RMA) analysis.[29] For identification of previously undescribed transcripts differentially regulated during prion disease, probe sets from the prion infection time course were filtered on expression (10.0–99.0th expression percentile) and statistically assessed using one-way ANOVA analysis (post hoc Tukey HSD and Benjamini-Hochberg correction; $p \leq 0.05$) and further filtered by ≥1.5 fold expression. The cuprizone treatment data set was also filtered on expression (10.0–99.0th expression percentile) and subjected to unpaired t-test analysis (Benjamini-Hochberg correction; $p \leq 0.05$) and further filtering by ≥1.5 fold expression against control.

For comparative analysis, the data sets from the prion infection time course were re-analyzed by filtering on expression (10.0–99.0th expression percentile) and clustering using 3 x 4 Self-Organizing Map (SOM) analysis. One cluster contained transcripts whose expression increased during the course of prion disease; these transcripts were statistically assessed using one-way ANOVA analysis (post hoc Tukey HSD and Benjamini-Hochberg correction; $p \leq 0.05$) and further filtered by ≥1.5 fold expression. Transcripts from the cuprizone data set with no expression change between control and cuprizone treatment were identified using the Euclidean similarity metric (a coefficient of correlation 0.85–1.0). To categorize transcripts specific to prion disease (i.e., not associated with cuprizone-induced neuroinflammation), the prion time course dataset was compared to the unchanging cuprizone dataset. Probe sets present in both analyses are transcripts upregulated during prion disease and unchanged with cuprizone treatment. Annotational

information and gene ontology biological functions were determined using the DAVID functional annotation database.[30]

Staining and immunohistochemistry. Ten micron thick sagittal cryo-sections were cut and placed on glass slides for staining or immunohistochemistry (IHC). Slides were stained with hematoxylin and eosin (H&E) for histological detection of vacuolation. For IHC, slides were prepared as previously described[31] with minor variations. Slides were incubated with primary antibody of either anti-GFAP (Promega Co., Madison, WI) or anti-prion protein, [SAF-83] (Cayman Chemical, Ann Arbor, Michigan), diluted 1:500 or 1:1,000, respectively, overnight at 4°C. After washing, the sections were incubated with biotinylated secondary antibody anti-rabbit IgG (1:200) for 1 h at room temperature, washed again and the antibody complex was detected using 3,3'-diaminobenzidine (DAB) (Sigma-Aldrich, St. Louis, MO) for GFAP or 3-amino-9-ethyl-carbazole (AEC) (Vector Laboratories, Burlingame, CA) for prion protein, according to manufacturer's protocol.

Quantitative RT-PCR. cDNA was created as described above from total RNA isolated from mouse brain homogenates for additional PCR amplification using iQ Sybr Green Supermix (BioRad, Hercules, CA). The PCR amplification cycle varied with each gene being amplified (Suppl. Table 1). Relative expression values were determined using the iCycler software package and Pfaffl analysis using *Tbp* as the housekeeping gene for normalization.[32]

Acknowledgements

We would like to thank Debbie McKenzie (University of Alberta) for helpful discussion and assistance in manuscript preparation and David Westaway (University of Alberta) for critical reading of the manuscript. This research was supported by NIH grant RO1 NS060034 (to Judd M. Aiken).

Note

Supplementary materials can be found at:
www.landesbioscience.com/supplement/MoodyPRION3-2-Sup.pdf

References

1. Collinge J. Prion diseases of humans and animals: Their causes and molecular basis. Annu Rev Neurosci 2001; 24:519-50.
2. Duguid JR, Rohwer RG, Seed B. Isolation of cDNAs of scrapie-modulated RNAs by subtractive hybridization of a cDNA library. Proc Natl Acad Sci USA 1988; 85:5738-42.
3. Duguid JR, Bohmont CW, Liu NG, Tourtellotte WW. Changes in brain gene expression shared by scrapie and alzheimer disease. Proc Natl Acad Sci USA 1989; 86:7260-4.
4. Duguid JR, Dinauer MC. Library subtraction of in vitro cDNA libraries to identify differentially expressed genes in scrapie infection. Nucleic Acids Res 1990; 18:2789-92.
5. Diedrich JF, Minnigan H, Carp RI, Whitaker JN, Race R, Frey W, 2nd, Haase AT. Neuropathological changes in scrapie and alzheimer's disease are associated with increased expression of apolipoprotein E and cathepsin D in astrocytes. J Virol 1991; 65:4759-68.
6. Duguid J, Trzepacz C. Major histocompatibility complex genes have an increased brain expression after scrapie infection. Proc Natl Acad Sci USA 1993; 90:114-7.
7. Diedrich JF, Carp RI, Haase AT. Increased expression of heat shock protein, transferrin and beta 2-microglobulin in astrocytes during scrapie. Microb Pathog 1993; 15:1-6.
8. Dandoy-Dron F, Guillo F, Benboudjema L, Deslys JP, Lasmezas C, Dormont D, et al. Gene expression in scrapie. cloning of a new scrapie-responsive gene and the identification of increased levels of seven other mRNA transcripts. J Biol Chem 1998; 273:7691-7.
9. Baker CA, Manuelidis L. Unique inflammatory RNA profiles of microglia in creutzfeldt-jakob disease. Proc Natl Acad Sci USA 2003; 100:675-9.
10. Booth S, Bowman C, Baumgartner R, Dolenko B, Sorensen G, Robertson C, et al. Molecular classification of scrapie strains in mice using gene expression profiling. Biochem Biophys Res Commun 2004; 325:1339-45.
11. Booth S, Bowman C, Baumgartner R, Sorensen G, Robertson C, Coulthart M, et al. Identification of central nervous system genes involved in the host response to the scrapie agent during preclinical and clinical infection. J Gen Virol 2004; 85:3459-71.
12. Brown AR, Webb J, Rebus S, Williams A, Fazakerley JK. Identification of upregulated genes by array analysis in scrapie-infected mouse brains. Neuropathol Appl Neurobiol 2004; 30:555-67.
13. Riemer C, Neidhold S, Burwinkel M, Schwarz A, Schultz J, Kratzschmar J, et al. Gene expression profiling of scrapie-infected brain tissue. Biochem Biophys Res Commun 2004; 323:556-64.
14. Xiang W, Windl O, Wunsch G, Dugas M, Kohlmann A, Dierkes N, et al. Identification of differentially expressed genes in scrapie-infected mouse brains by using global gene expression technology. J Virol 2004; 78:11051-60.
15. Brown AR, Rebus S, McKimmie CS, Robertson K, Williams A, Fazakerley JK. Gene expression profiling of the preclinical scrapie-infected hippocampus. Biochem Biophys Res Commun 2005; 334:86-95.
16. Skinner PJ, Abbassi H, Chesebro B, Race RE, Reilly C, Haase AT. Gene expression alterations in brains of mice infected with three strains of scrapie. BMC Genomics 2006; 7:114.
17. Xiang W, Hummel M, Mitteregger G, Pace C, Windl O, Mansmann U, Kretzschmar HA. Transcriptome analysis reveals altered cholesterol metabolism during the neurodegeneration in mouse scrapie model. J Neurochem 2007; 102:834-47.
18. Williams AE, Lawson LJ, Perry VH, Fraser H. Characterization of the microglial response in murine scrapie. Neuropathol Appl Neurobiol 1994; 20:47-55.
19. DeArmond SJ, Kristensson K, Bowler RP. PrP^{Sc} causes nerve cell death and stimulates astrocyte proliferation: A paradox. Prog Brain Res 1992; 94:437-46.
20. Eikelenboom P, Bate C, Van Gool WA, Hoozemans JJ, Rozemuller JM, Veerhuis R, Williams A. Neuroinflammation in alzheimer's disease and prion disease. Glia 2002; 40:232-9.
21. McGeer PL, Itagaki S, Boyes BE, McGeer EG. Reactive microglia are positive for HLA-DR in the substantia nigra of parkinson's and alzheimer's disease brains. Neurology 1988; 38:1285-91.
22. Martino G, Adorini L, Rieckmann P, Hillert J, Kallmann B, Comi G, Filippi M. Inflammation in multiple sclerosis: The good, the bad and the complex. Lancet Neurol 2002; 1:499-509.
23. Greenwood AD, Horsch M, Stengel A, Vorberg I, Lutzny G, Maas E, et al. Cell line dependent RNA expression profiles of prion-infected mouse neuronal cells. J Mol Biol 2005; 349:487-500.
24. Blakemore WF. Observations on oligodendrocyte degeneration, the resolution of status spongiosus and remyelination in cuprizone intoxication in mice. J Neurocytol 1972; 1:413-26.
25. Ludwin SK. Central nervous system demyelination and remyelination in the mouse: An ultrastructural study of cuprizone toxicity. Lab Invest 1978; 39:597-612.
26. Pattison IH, Jebbett JN. Histopathological similarities between scrapie and cuprizone toxicity in mice. Nature 1971; 230:115-7.
27. Hiremath MM, Saito Y, Knapp GW, Ting JP, Suzuki K, Matsushima GK. Microglial/macrophage accumulation during cuprizone-induced demyelination in C57BL/6 mice. J Neuroimmunol 1998; 92:38-49.
28. Bakker DA, Ludwin SK. Blood-brain barrier permeability during cuprizone-induced demyelination. implications for the pathogenesis of immune-mediated demyelinating diseases. J Neurol Sci 1987; 78:125-37.
29. Irizarry RA, Hobbs B, Collin F, Beazer-Barclay YD, Antonellis KJ, Scherf U, Speed TP. Exploration, normalization and summaries of high density oligonucleotide array probe level data. Biostatistics 2003; 4:249-64.
30. Dennis G Jr, Sherman BT, Hosack DA, Yang J, Gao W, Lane HC, Lempicki RA. DAVID: Database for annotation, visualization and integrated discovery. Genome Biol 2003; 4:3.
31. Hoefert VB, Aiken JM, McKenzie D, Johnson CJ. Labeling of the scrapie-associated prion protein in vitro and in vivo. Neurosci Lett 2004; 371:176-80.
32. Pfaffl MW. A new mathematical model for relative quantification in real-time RT-PCR. Nucleic Acids Res 2001; 29:45.
33. Lee CK, Weindruch R, Prolla TA. Gene-expression profile of the ageing brain in mice. Nat Genet 2000; 25:294-7.
34. Lewicki H, Tishon A, Homann D, Mazarguil H, Laval F, Asensio VC, et al. T cells infiltrate the brain in murine and human transmissible spongiform encephalopathies. J Virol 2003; 77:3799-808.
35. Porter DD, Porter HG, Cox NA. Failure to demonstrate a humoral immune response to scrapie infection in mice. J Immunol 1973; 111:1407-10.
36. Roberts ES, Zandonatti MA, Watry DD, Madden LJ, Henriksen SJ, Taffe MA, Fox HS. Induction of pathogenic sets of genes in macrophages and neurons in NeuroAIDS. Am J Pathol 2003; 162:2041-57.
37. Moore KJ, El Khoury J, Medeiros LA, Terada K, Geula C, Luster AD, Freeman MW. A CD36-initiated signaling cascade mediates inflammatory effects of beta-amyloid. J Biol Chem 2002; 277:47373-9.

38. Morell P, Barrett CV, Mason JL, Toews AD, Hostettler JD, Knapp GW, Matsushima GK. Gene expression in brain during cuprizone-induced demyelination and remyelination. Mol Cell Neurosci 1998; 12:220-7.
39. Arnett HA, Wang Y, Matsushima GK, Suzuki K, Ting JP. Functional genomic analysis of remyelination reveals importance of inflammation in oligodendrocyte regeneration. J Neurosci 2003; 23:9824-32.
40. Jurevics H, Largent C, Hostettler J, Sammond DW, Matsushima GK, Kleindienst A, et al. Alterations in metabolism and gene expression in brain regions during cuprizone-induced demyelination and remyelination. J Neurochem 2002; 82:126-36.
41. Bedard A, Tremblay P, Chernomoretz A, Vallieres L. Identification of genes preferentially expressed by microglia and upregulated during cuprizone-induced inflammation. Glia 2007; 55:777-89.
42. Lopez I, Mak EC, Ding J, Hamm HE, Lomasney JW. A novel bifunctional phospholipase c that is regulated by galpha 12 and stimulates the Ras/mitogen-activated protein kinase pathway. J Biol Chem 2001; 276:2758-65.
43. Shutter JR, Graham M, Kinsey AC, Scully S, Luthy R, Stark KL. Hypothalamic expression of ART, a novel gene related to agouti, is upregulated in obese and diabetic mutant mice. Genes Dev 1997; 11:593-602.
44. Ollmann MM, Wilson BD, Yang YK, Kerns JA, Chen Y, Gantz I, Barsh GS. Antagonism of central melanocortin receptors in vitro and in vivo by agouti-related protein. Science 1997; 278:135-8.
45. Guzik TJ, Mangalat D, Korbut R. Adipocytokines—novel link between inflammation and vascular function? J Physiol Pharmacol 2006; 57:505-28.
46. Watson RT, Khan AH, Furukawa M, Hou JC, Li L, Kanzaki M, et al. Entry of newly synthesized GLUT4 into the insulin-responsive storage compartment is GGA dependent. EMBO J 2004; 23:2059-70.
47. Emanuelli B, Peraldi P, Filloux C, Sawka-Verhelle D, Hilton D, Van Obberghen E. SOCS-3 is an insulin-induced negative regulator of insulin signaling. J Biol Chem 2000; 275:15985-91.